Climatology of the stratospheric BrO vertical distribution by balloon-borne UV–visible spectrometry

I. Pundt,[1,2] J.-P. Pommereau,[1] M. P. Chipperfield,[3] M. Van Roozendael,[4] and F. Goutail[1]

Received 25 February 2002; revised 7 July 2002; accepted 16 August 2002; published 28 December 2002.

[1] A balloon-borne UV–visible spectrometer, the SAOZ-BrO, has been designed for the measurement of BrO on small and relatively low-cost balloons. It allows the retrieval of the vertical BrO profile with a resolution of 1 km, a precision of 0.5–2 pptv (below 25 km), and a +5/−10% accuracy during the daytime balloon ascent. Fifteen successful flights have been carried out since 1997. Significant BrO amounts were observed at all latitudes and seasons, with a peak concentration altitude varying from 15 km in the winter vortex to 22 km in the tropics. The mixing ratio increases steadily from the tropopause to 25–30 km, depending on the latitude, above which it remains constant up to 30 km. The latitudinal and seasonal changes (maximum at high latitude and in the winter) are largely controlled by the vertical transport of total inorganic bromine and to a smaller extent by photochemistry. Photochemical changes are primarily related to NO_2 abundances. On a constant potential temperature surface, the BrO mixing ratio is the largest in Polar Regions in the winter, where NO_2 is nearly absent. In contrast, BrO is the smallest during the polar day and in the summer at midlatitude. The presence of activated chlorine in the cold vortex has little impact on BrO abundances. Finally, significant amounts were observed in the upper troposphere: (1) in the summer at midlatitude where it was the result of a stratosphere–troposphere exchange (STE) event advecting bromine from the stratosphere and (2) at the tropics where its presence is likely due to the conversion of organic bromine at lower altitude. *INDEX TERMS:* 0340 Atmospheric Composition and Structure: Middle atmosphere—composition and chemistry; 0394 Atmospheric Composition and Structure: Instruments and techniques; 1640 Global Change: Remote sensing; *KEYWORDS:* Stratosphere, chemistry, bromine, Climatology, balloon, UV–visible spectrometry

Citation: Pundt, I., J.-P. Pommereau, M. P. Chipperfield, M. Van Roozendael, and F. Goutail, Climatology of the stratospheric BrO vertical distribution by balloon-borne UV–visible spectrometry, *J. Geophys. Res.*, *107*(D24), 4806, doi:10.1029/2002JD002230, 2002.

1. Introduction

[2] Bromine has long been identified as contributing to ozone destruction in the polar stratosphere by a catalytic cycle involving also ClO, the ClO–BrO cycle [*McElroy et al.*, 1986]. However, because BrO is anticipated to be a dominant form of inorganic bromine at all latitudes and seasons, it has the potential to destroy ozone also at midlatitudes [*Wofsy et al.*, 1975; *Yung et al.*, 1980; *Garcia and Solomon*, 1994; *Wennberg et al.*, 1994; *Lary et al.*, 1996; *Daniel et al.*, 1999] and possibly also at the tropics.

[3] The sources of inorganic bromine in the stratosphere are about one third from natural marine and terrestrial methyl bromide (CH_3Br), and about two-thirds from anthropogenic methyl bromide and Halons emitted at the surface [*WMO Reports*, 1995, 1999]. When transported to higher altitudes in the troposphere and the stratosphere, they are converted into inorganic forms ($Br_Y = Br + BrO + HOBr + BrONO_2 + HBr + BrCl$) by photolysis or reaction with OH radicals. From organic bromine measurements, the total stratospheric bromine abundance has been estimated as 16 ± 2 pptv in air, which entered the stratosphere in 1994 [*Wamsley et al.*, 1998], and 17.4 ± 0.9 pptv in air, which entered the stratosphere in 1996 [*Schauffler et al.*, 1998], respectively. Due to continuing Halon emission, total bromine would have increased by about 3 pptv during one decade [e.g., *Wamsley et al.*, 1998; *Fraser et al.*, 1999]. In addition, it has been proposed that significant amounts of inorganic bromine could be present in the free troposphere and transported into the stratosphere [e.g., *Ko et al.*, 1997], leading to higher total bromine amounts in the stratosphere [*Dvortsov et al.*, 1999; *Schauffler et al.*, 1999; *Sturges et al.*, 2000; *Pfeilsticker et al.*, 2000]. Indeed, BrO concentrations of the order of 1–3 pptv have been observed in the free troposphere [e.g., *Van Roozendael et al.*, 2002; *McElroy et al.*, 1999; *Pundt et al.*, 2000; *Fitzenberger et al.*, 2000]. Overall, the transport of organic and inorganic bromine from the troposphere would imply a total stratospheric bromine burden of 17–22 pptv for air entering the stratosphere in 1996, as also concluded by *Harder et al.* [2000].

[1]Service d'Aéronomie, CNRS, Verrières-le-Buisson, France.
[2]Now at Institute of Environmental Physics, University of Heidelberg, Im Neuenheimer Feld 229, 69120 Heidelberg, Germany.
[3]School of the Environment, University of Leeds, Leeds, UK.
[4]Belgian Institute for Space Aeronomy, Brussels, Belgium.

0148-0227/02/2002JD002230

[4] The partitioning between bromine species is still subject to speculation, since only BrO has been routinely observed, while a few measurements of stratospheric HBr and an upper limit of HOBr [*Johnson et al.*, 1995; *Nolt et al.*, 1997] are available only. The other species, Br, $BrONO_2$, and BrCl, have never been observed. Photochemical model simulations suggest that nearly all stratospheric Br_Y is in the form of BrO, $BrONO_2$, and HOBr (and BrCl if chlorine is activated) and that BrO, the ozone-depleting compound, could represent about 30–70% of the total Br_Y during daytime [*Lary*, 1996; *Sinnhuber et al.*, 2002]. This is in agreement with the observations of *Avallone et al.* [1995] indicating that BrO could represent 40% of Br_Y.

[5] Most of the experimental information on stratospheric bromine thus comes from BrO. It has been measured for more than a decade by two different methods; in situ by resonance fluorescence, a method pioneered by *Brune and Anderson* [1986] and remotely as integrated column density by UV–visible spectroscopy after *Carroll et al.* [1989]. In addition, BrO abundances have also been estimated indirectly via spectroscopic measurements of OClO [*Solomon et al.*, 1989]. Indeed OClO is formed through the reaction of BrO with ClO and is therefore an indicator for the presence of both species.

[6] Slant column densities of BrO are now measured continuously by UV–visible zenith-sky spectroscopy from a number of ground-based stations [*Carroll et al.*, 1989; *Solomon et al.*, 1989; *Fish et al.*, 1997; *Richter et al.*, 1999; *Otten et al.*, 1998; *Friess et al.*, 1999; *Sinnhuber et al.*, 2002], and, since 1995, from space by the GOME instrument on board the ESA ERS-2 satellite [*Wagner and Platt*, 1998; *Richter et al.*, 2002; *Hegels et al.*, 1998; *Burrows et al.*, 1999a]. Column measurements have been also performed from aircraft [*Wahner et al.*, 1990; *Grendel et al.*, 1996].

[7] The ground-based twilight measurements report significant BrO column amounts from middle to high latitudes in both hemispheres with, however, significant seasonal and latitudinal variations. The column density is larger in the winter and at high latitudes compared to the midlatitude summer [*Arpag et al.*, 1994; *Fish et al.*, 1997; *Richter et al.*, 1999; *Kreher et al.*, 1997; *Otten et al.*, 1998; *Sinnhuber et al.*, 2002]. Global noontime observations by GOME reveal similar latitudinal and seasonal variations, although the BrO total column seen by GOME also includes a tropospheric contribution which dominates the signal in polar regions at spring [*Wagner and Platt*, 1998; *Richter et al.*, 2001, 2002; *Wagner*, 1999]. Since the variation of the stratospheric column of BrO is found to be anticorrelated with that of NO_2 measured by the same instruments, it has been suggested that the amount of BrO is largely controlled by NO_2, which converts BrO into $BrONO_2$ [*Fish et al.*, 1997; *Richter et al.*, 1999]. Regarding the influence of chlorine, the information is more controversial since some authors do report an increase of the column inside the vortex [*Aliwell et al.*, 1997; *Otten et al.*, 1998], while others do not [*Grendel et al.*, 1996; *Richter et al.*, 1999].

[8] The number of in situ measurements in the stratosphere is more limited. Local concentrations at the cruise altitude of the NASA ER-2 aircraft (around 19–20 km) have been measured by resonance–fluorescence over Antarctica [*Brune et al.*, 1989] and at middle and low latitudes [*Avallone et al.*, 1995], indicating a latitudinal increase of the BrO mixing ratio toward the Arctic in February. As in the case of the total column, some measurements reveal increased BrO mixing ratios in the vortex [*Brune et al.*, 1989; *Toohey et al.*, 1990]. Other do not [*Avallone et al.*, 1995], however, this could be result of the impact of volcanic aerosols since the measurements were carried out little after the eruption of Mount Pinatubo when the NO_x concentration was significantly reduced at midlatitude and not yet in the vortex.

[9] Finally, some information on the vertical distribution of BrO is also available from ER-2 aircraft dives in the lower stratosphere [*Brune and Anderson*, 1986; *Toohey et al.*, 1990] and from balloon using the same resonance–fluorescence technique [*McKinney et al.*, 1997; *Stroh et al.*, 1998] and UV–visible spectroscopy [*Pundt et al.*, 1997; *Harder et al.*, 1998]. Recently, a BrO profile was also measured remotely by submillimeter infrared emission spectroscopy from a Falcon aircraft [*Hetzheim et al.*, 1998]. All measurements suggest that the BrO mixing ratio increases with altitude in the stratosphere at all latitudes to reach a maximum of 8–15 pptv around 25–30 km.

[10] In summary, the observation of atmospheric BrO has improved rapidly during recent years. However, still little information is available on its vertical distribution, a prerequisite for the understanding of problems such as the relative role of transport and chemistry on the observed seasonal and latitudinal changes, the impact of a possible tropospheric source on the stratosphere, the respective role of chlorine and NO_x species in the partitioning of total inorganic bromine and, finally, the overall impact of bromine on ozone.

[11] Here we report on the measurement of a series of 15 BrO profiles from 10 to 30 km carried out during daytime at all latitudes in the winter and the summer between 1997 and 2000 using a balloon-borne SAOZ UV–visible spectrometer specially adapted for BrO. From this data set, a first climatology of the vertical distribution of BrO will be derived which could be used to investigate the influence of transport, NO_x chemistry, and chlorine activation on bromine in the stratosphere and the upper troposphere.

[12] The paper is organized in two parts. First, section 2 provides a full description of the instrument, the spectral analysis and profile retrieval and, finally, the precision and accuracy of the measurements. After giving the required information on the balloon flights, a summary of the BrO profiles is presented in section 3, followed by a detailed discussion of each latitude and season combining the BrO observations with the temperature, ozone, NO_2 and OClO data provided by the regular SAOZ sonde flown simultaneously on the same balloon.

2. The Measurement of BrO With the SAOZ-BrO Balloon Sonde

[13] The SAOZ-BrO balloon experiment is a lightweight UV optical sonde specifically designed for the measurement of BrO, as well as other UV-absorbing species such as OClO and CH_2O, by solar occultation from small and relatively inexpensive balloons [*Pommereau et al.*, 1999]. The instrument and the payload are derived from the SAOZ UV–visible sonde, flown more than 100 times since 1992, which measures ozone, NO_2, OClO, $(O_2)_2$, H_2O, and the upper limit of IO at a variety of latitudes [*Pommereau and*

Table 1. Optical Characteristics of the Two Versions of the SAOZ Spectrometer

Sonde	Groves/ mm	Entrance slit (μm)	Dispersion (nm/pixel)	FWHM (nm)	Filter
SAOZ UV/Visible	360	50	0.5	1	-
SAOZ-BrO	1200	250	0.08	0.9	UG 5

Piquard, 1994a, 1994b; *Pundt et al.*, 1998; *Goutail et al.*, 1999]. The data are spectrally analyzed by the DOAS (Differential Optical Absorption Spectroscopy) method [e.g., *Platt*, 1994] and vertical profiles of the species are retrieved by an onion peeling procedure.

2.1. The SAOZ-BrO Sonde

[14] SAOZ-BrO is similar in all aspects to the regular SAOZ sonde (i.e., no Sun tracker but light collector of 360° azimuth and −5°/+15° elevation FOV, 1024 diode array detector, autonomous measurement sequence driven by an onboard CPU, mechanical and thermal protection, Global Positioning System (GPS) and meteorological sensors), except for two elements: the spectrometer and the optical entrance. The spectrometer performances have been improved in the ultraviolet part of the spectrum to enhance the sensitivity of the instrument to the weak BrO absorption bands.

[15] The FWHM of the slit function is sampled by 10 diodes instead of 3 in the regular version using a more dispersive grating (1200 grooves/mm) at the expense of a reduction of the spectral range to 320–400 nm. The entrance slit has been enlarged to 250 μm to maintain the spectral resolution (0.9 nm FWHM) and a filter has been added to reduce the straylight from longer wavelengths. For comparison, the optical characteristics of both spectrometers are summarized in Table 1.

[16] The second change, now in use in all SAOZ sondes, is the replacement of the optical head at the entrance by a more diffusive one [*Pundt*, 1997]. This has been made necessary for minimizing the small spectral shifts associated to the rotation of the gondola and thus of the entrance slit with respect to the direction of the Sun. Indeed this effect, proved to be difficult to correct, is resulting in small spectral features interfering with the signature of the absorbers. The new arrangement is shown in Figure 1. Sunlight is reflected by a conical mirror onto a system of three quartz diffusers of decreasing size mounted into a reflective cone, whose role is to concentrate and mix the optical rays before entering into the slit of the spectrometer. This system allowed the reduction of the spectral shifts associated with the rotation of the payload to less than 0.05 pixels resulting in a negligible impact on spectral features. In addition, the remaining wavelength shift and change in slit function are smoothed out by the rotation of the gondola (1 turn/3 s on average during the ascent of the balloon).

[17] As in the case of the conventional SAOZ, the spectrometer is neither thermostated nor pressurized. The cooling of −8/−10 K along a 3 h flight and the pressure reduction from 1000 to 10 hPa also result in a slow varying spectral shift, which partly compensate because of their opposite direction. The maximum shift is 0.2 pixels (or

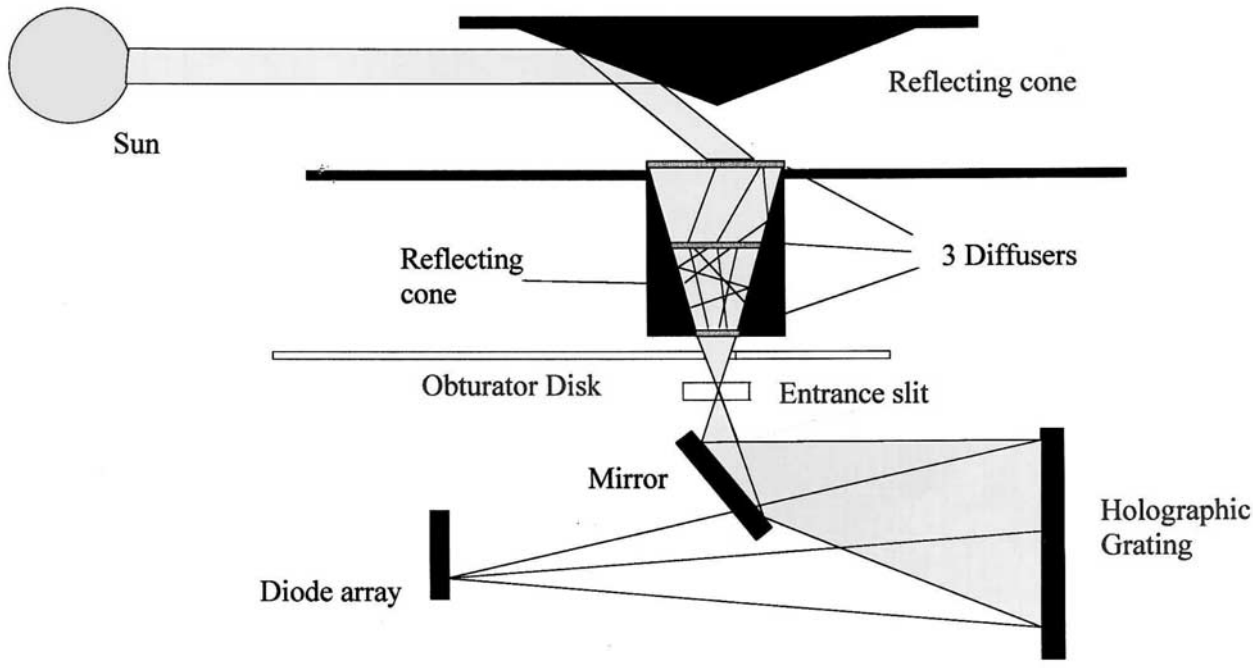

Figure 1. Optical layout of the SAOZ balloon sonde since 1994 [*Pundt*, 1997]. The light coming from different directions (−5, +15° elevation and 0°–360° azimuth) is reflected by an aluminized cone pointing downward, concentrated, and mixed by a set of three diffuser plates mounted into a second reflecting cone. The distance and height of the lowest diffuser plate in front of the entrance slit are adjusted to the aperture of the spectrometer.

Table 2. Source of Molecular Absorption Cross Sections, Temperature, I_0 Correction, and Spectral Shift Used in the Spectral Analysis Following the Recommendations of *Aliwell et al.* [2002]

Species	Reference	Temp.	I_0 corr (mol/cm^2)	Shift (nm)
Ozone	*Burrows et al.* [1999b]	221 K	1e20	0.03
Ozone	*Burrows et al.* [1999b]	241 K	1e20	0.03
NO_2	*Van Daele et al.* [1998]	220 K	5e16	0
BrO	*Wahner et al.* [1988]	223 K	0	0.17
OClO	*Wahner et al.* [1987]	204 K	0	0
O_4	*Hermans et al.* [2000][a]	ambient	0.005	0

[a] Hermans et al. (Absorption bands of O_2 and its collision-induced bands in the 30,000–7500 cm^{-1} wavenumber region, *Proceedings of IRS 2000, St. Petersburg, Russia, July 24–25*, submitted, 2000. Data available from http://www.oma.be/BIRA-IASB/Scientific/Data/CrossSections/CrossSectionst.html).

0.016 nm) during the reported periods of the flights, which is easily corrected by the wavelength alignment procedure of the spectral analysis algorithm described below.

2.2. Spectral Analysis

[18] The spectral analysis is made by the DOAS technique using the WINDOAS algorithm developed at the Belgian Institute for Space Aeronomy [*Van Roozendael et al.*, 1999]. It includes all recommendations defined after a BrO intercomparison campaign held at the Observatoire de Haute Provence in 1996, described by *Aliwell et al.* [2002]. The software used in the present analyses is therefore fully consistent with that in use at the various NDSC ground-based stations as well as in the analysis of the GOME ERS-2 satellite data.

[19] In this procedure, atmospheric spectra are aligned in wavelength and ratioed to a reference spectrum corresponding to the minimum residual atmospheric absorption during the flight, generally the first recorded after reaching float. The absolute wavelength calibration is obtained by comparison to the Kitt Peak reference solar spectrum [*Kurucz et al.*, 1984]. The resulting atmospheric attenuation spectra are then analyzed by comparison with the absorption cross sections of the species using a multiparameter nonlinear least squares fit procedure, providing the column density of the absorber and its one sigma uncertainty, used as a measure of the precision. The source of the absorption cross sections, their temperature, the scaling factor used for the I_0 correction (see below) and the wavelength shift applied, are listed in Table 2. The highly resolved laboratory absorption cross sections are adapted to the resolution of the spectrometer by convolution with its slit function measured with a mercury lamp. The slit function measured by several adjacent mercury lines is constant in the 330–370 nm range.

[20] Our experience suggests that the most sensitive parameter in the measurement of BrO are, if not corrected for: the solar I_0 correction of the cross sections, the removal of the temperature-dependent ozone absorption (10 times larger than that of BrO), and the temperature dependence of the BrO absorption cross sections. The solar I_0 effect arises because of the difference in the absorption features of the trace gases measured in the laboratory with a spectrally smooth light source and in the atmosphere using the highly structured solar light (Johnston, unpublished results). A procedure has been suggested for correcting the cross sections [*Aliwell et al.*, 2002] and applied here to ozone, NO_2 and O_4. The temperature dependence of the ozone cross sections is accounted for by a linear fitting of two sets of cross sections measured at two different stratospheric temperatures (221 K and at 241 K) [*Aliwell et al.*, 2002].

[21] The BrO cross sections are those measured by *Wahner et al.* [1988] at 223 K (quoted accuracy 5%). However, since newer cross sections reported by *Gilles et al.* [1997] are 10% larger, we will adopt a conservative uncertainty of −5/+10%. In addition, the amplitude of the bands increases at decreasing temperature. A linear extrapolation of the two Wahner's determinations at 223 and 298 K suggests that the column density could be reduced by 12% at 195 K compared to that calculated using cross sections at 223 K. However, since this temperature dependence is uncertain, no systematic correction has been applied, but the factor will be taken into account in the discussion of the results in the Arctic winter.

[22] As an example, Figure 2 shows the results of the analysis of a spectrum recorded on 20 March 1997 in the polar vortex over Kiruna in Northern Sweden at an altitude of 10 km during the daytime ascent of the balloon at 84° SZA. Note the large range of left-hand scales: 0.2 for ozone and a few 10^{-3} for the other absorbents. NO_2 and OClO are almost absent. The stratospheric NO_2 concentration is very small in the still cold vortex, and though

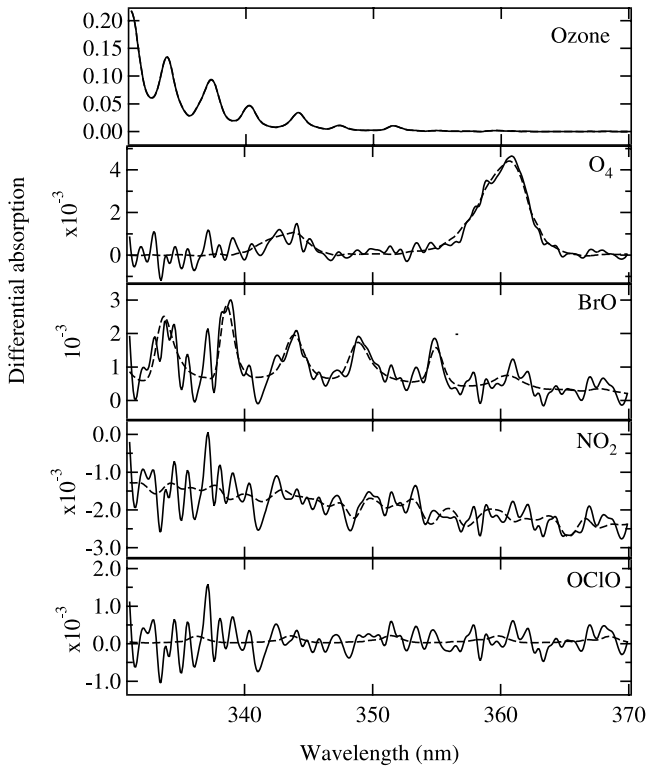

Figure 2. Example of analysis for a spectrum recorded during the balloon ascent at an altitude of 10 km and 84° SZA on 20 March 1997 in the winter polar vortex over Kiruna. Full lines: atmospheric absorption; dotted: laboratory cross sections. From top to bottom: ozone, O_4, BrO, NO_2, and OClO. BrO is measured on 5 consecutive bands.

chlorine is activated, OClO that forms at sunset is absent during daytime.

[23] Though noisier at wavelengths shorter than 338 nm, the analysis can be extended over the 331–370 nm region. This allows the measurement of BrO on five absorption bands instead of two in the conventional 345–360 nm region used for example by ground-based instruments. The advantage is a better removal of possible interferences with other species or residual features related from artifacts related to Fraunhofer absorption lines and wavelength shift artifacts. The residual structures are enhanced at shorter wavelengths, due to the worse removal of the ozone structures and higher noise level. However, the derived slant column amounts are similar to those obtained by using two bands only.

2.3. Analysis of Flight Data

[24] The spectral analysis results in a series of slant column densities and random errors of the various species along the flight. These are converted into vertical profiles by a linear onion peeling inversion procedure using the altitude and location provided by the GPS for calculating the tangent height of the solar beam after correction for atmospheric refraction.

2.3.1. Slant Column Density

[25] The evolution of the slant columns of O_4, O_3, BrO, OClO, and NO_2, during the flight from which the spectral fit shown in Figure 2 was taken, is displayed in Figure 3, together with the altitude of the balloon, the solar zenith angle and the tangent height during the occultation period (at SZA < 90°, the tangent height becomes the minimum altitude of the solar beam which is the altitude of the balloon). Also shown is the color index, the ratio between irradiances measured at 550 nm and 350 nm by the conventional SAOZ also carried by the balloon, which will be used as an indicator of the contribution of scattered light and the presence of clouds. Error bars indicate the standard deviation of the least squares spectral fit, which is a measure of the precision.

[26] The balloon was launched in the afternoon in order to reach float at 30 km before sunset at SZA = 90°. Useful measurements could be obtained from the cloud top until about 92°–93° SZA from float altitude. In contrast to the conventional SAOZ in the visible where observations can be continued down to 10 or 12 km at occultation, the measurements must be stopped at 15–16 km in the UV because of the very large attenuation by ozone as well as the increase of scattered light compared to direct sunlight. The presence of clouds or the relative increase of scattered light can be seen readily by a drop (bluing) in the CI at the beginning of the flight. The measurements are then no longer useful.

[27] O_4 or $(O_2)_2$, the oxygen collision complex whose density is proportional to the square of $[O_2]$, only displays a significant absorption during the balloon ascent, below 15 km. The ozone column increases with SZA during ascent until 17 km around its peak concentration, above, which the column drops. It increases again rapidly when the Sun sets because of the rapidly increasing atmospheric path. NO_2 is detected but, since its maximum concentration is located at a higher altitude than that of ozone, its maximum during the ascent is shifted upward and its sunset increase starts earlier. In the example shown, the NO_2 column density remains very small below 20 km due to the large denoxification of the cold vortex. OClO remains also small, at the limit of significance during ascent, but increases relatively fast at sunset compared to others species. Almost absent during daytime due to its fast photolysis, OClO forms rapidly at sunset by reaction of BrO + ClO.

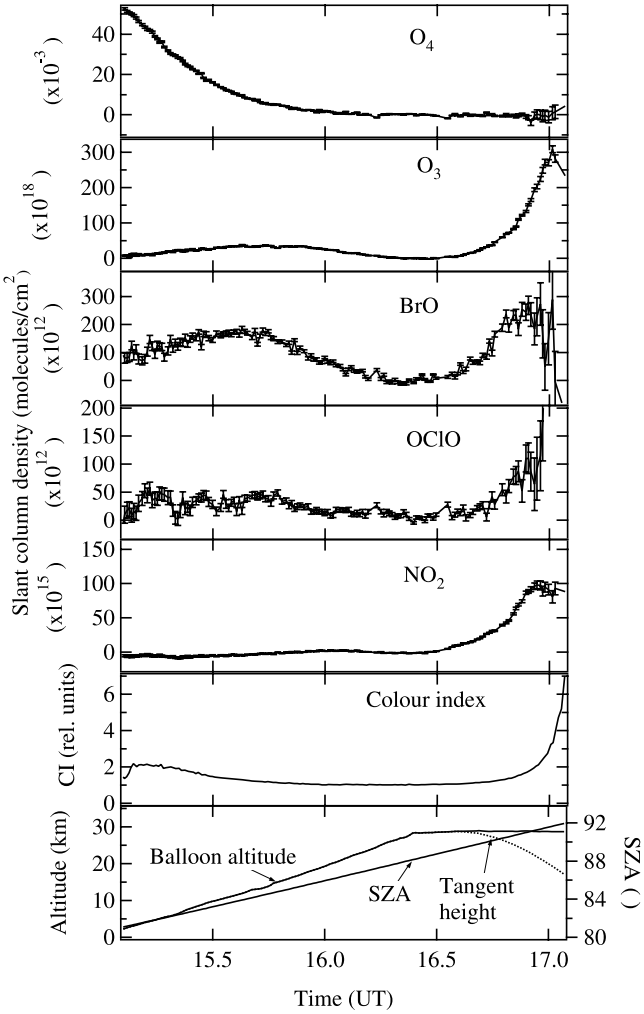

Figure 3. Slant column of absorbing species during the flight 20 March 1997. From top to bottom: O_4, O_3, BrO, OClO, and NO_2 with 1 s.d. error bars Color Index, and solar zenith angle (SZA), balloon altitude, and tangent height during occultation.

[28] Finally, BrO is in contrast with all other species. Its maximum slant column during ascent occurs around 14 km indicative of an altitude of its peak concentration lower than that of ozone, but the amplitude of its enhancement during occultation is relatively limited compared to that of the ascent. BrO is a daytime species. It converts to $BrONO_2$ at sunset except in chlorine activated conditions in the Arctic winter where the dominant bromine reservoir becomes BrCl. A reliable BrO measurement in the lower stratosphere could therefore be obtained only during daytime from the data recorded during the balloon ascent. Consequently, only daytime ascent measurements will be used for BrO in the following, while the O_3, NO_2 and OClO profiles used in the discussion will be those derived from the more sensitive measurements at occultation by the SAOZ regular sonde always flown together with the SAOZ-BrO payload.

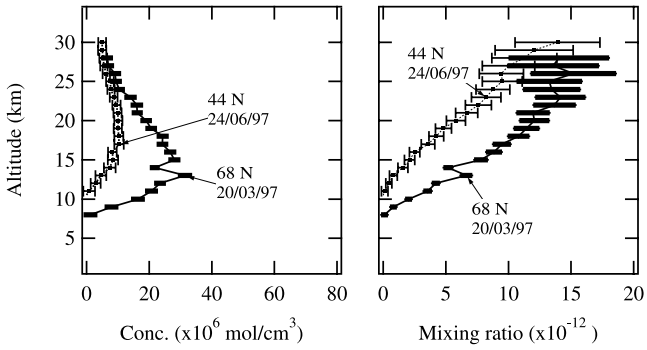

Figure 4. Vertical profile of BrO concentration on 20 March 1997 and 24 June 1997 retrieved by linear onion peeling from slant columns shown in Figure 3. The error bars indicate the uncertainty due to the unknown BrO amount above the balloon float altitude.

2.3.2. Profile Retrieval

[29] BrO number density profiles and associated random errors are retrieved by onion peeling after calculating the tangent height from GPS information (±100 m), including correction for refraction. Since the atmosphere in the retrieval process is divided into 1 km thick layers, and the vertical sampling of the measurements is 200 m during ascent and 300–1000 m during occultation, the data are smoothed with a 1 km broad filter. However, since the full solar disk is observed, the vertical resolution of the measurements is limited to 1.4 km.

[30] There are three specific aspects relevant to BrO which introduce some complication in the process: (1) the difficulty of determining the residual amount of BrO in the reference spectrum, (2) the BrO photochemical change during the 1 hour 20 min required for the ascent of the balloon, and (3) the possible contribution of light scattered by the atmosphere larger in the UV than in the visible.

[31] The inversion process requires first an assumption on the residual amount of the species in the reference spectrum recorded at float. For ozone and NO_2 this can be made to a high degree of precision by adjusting the residual from the comparison between ascent and occultation profiles in their upper part, since the atmospheric path length are very different and the chemical change of the constituent during the period is small (the NO_2 concentration does not increase significantly at sunset in the stratosphere before 93° SZA). For O_4, H_2O, or OClO, the residual could be set to zero, since the column density of these species above 3 km can be

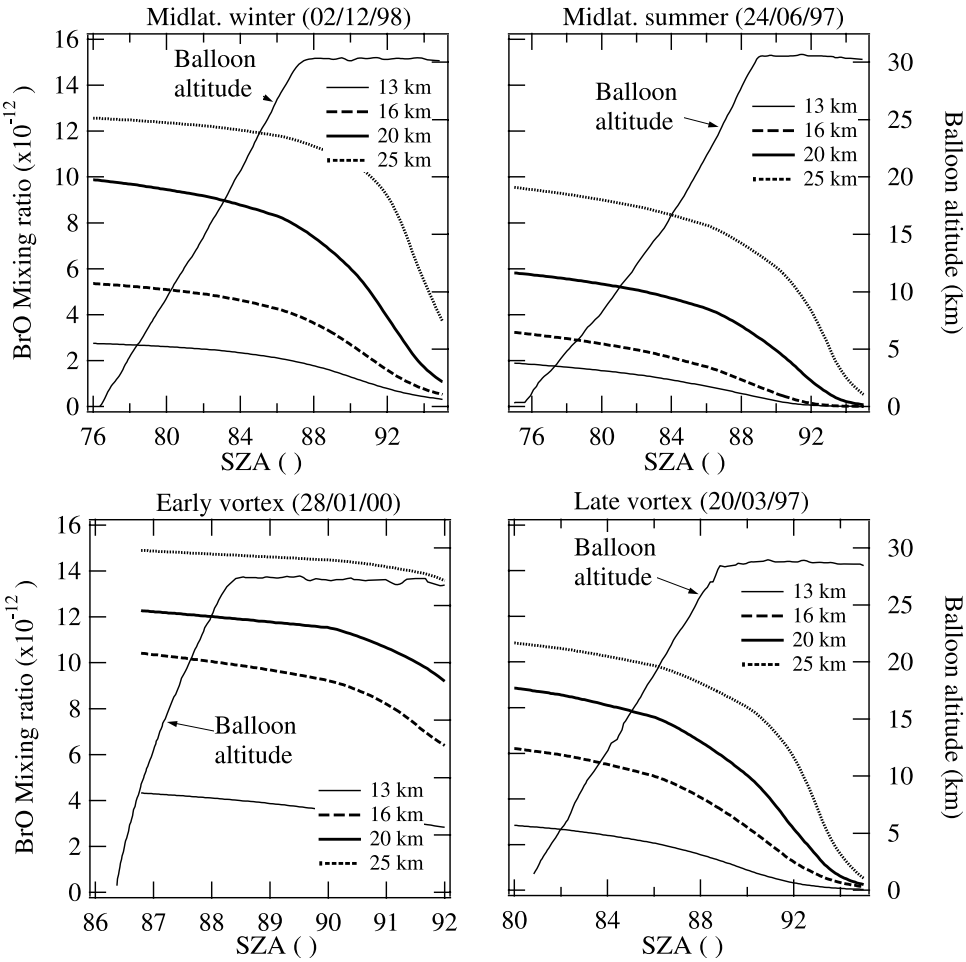

Figure 5. Simulation of BrO photochemical change in the afternoon at four altitude levels over Gap on 24 June 1997, Aire sur l'Adour on 2 December 1998, Kiruna on 20 March 1997, and Kiruna on 28 January 2000.

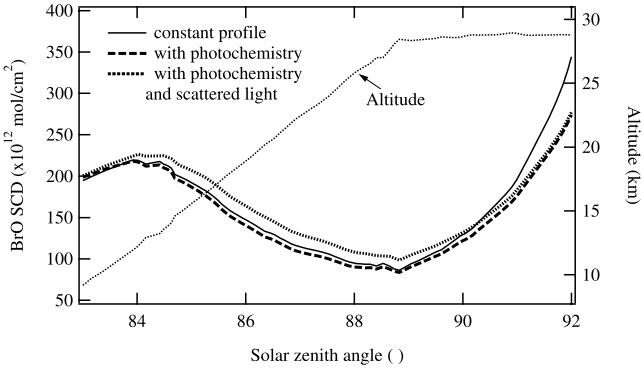

Figure 6. Simulation of impact of chemical change and scattered light on BrO slant columns for the flight of 20 March 1997 at Kiruna: (a) modeled BrO profile at 81° SZA (solid line), (b) photochemical change included (dashed), and (c) scattered light and photochemical change included (dotted).

neglected. For BrO the estimation of the residual is more difficult because BrO is still present above the maximum altitude of the balloon, dropping rapidly at sunset when the occultation starts. Since the method used for O_3 and NO_2 cannot provide more than a lower limit, the procedure used is to assume a constant mixing ratio of 18 pptv above the balloon which is larger than all estimations, and then defines an upper limit for the residual amount. Figure 4 shows two examples of profiles retrieved in the winter at Kiruna and in the summer in France together with error bars resulting from the difference between the two determinations of the residual amount. The uncertainty arising from the BrO residual column has a significant impact in the upper part of the profile (above 25 km) but its contribution drops rapidly at lower altitude, especially in units of mixing ratio, where it drops from 3 to 4 pptv down to less than 1 pptv at the bottom of the profile.

[32] The second concern in the BrO profile retrieval is the impact of the photochemical concentration changes during the measurements. Figure 5 shows the results of a Slimcat 1D model simulation of the photochemical change of the BrO concentration at four levels in the stratosphere in the afternoon for four different conditions: 2 December 1998 over Aire sur l'Adour, 24 June 1997 over Gap, and 28 January 2000 over Kiruna earlier in the season when NO_2 was almost absent and 20 March 1997. Also shown is the altitude of the balloon. The BrO concentration drops rapidly after 88°–89°. But the change during the ascent of the balloon is limited (5–10%) even in the Arctic when the Sun is already low (86°–87° SZA) when launch takes place. Indeed the Sun elevation varies very slowly at this latitude in the winter when the lift off occurs a little after noontime in the winter and a little before midnight in the summer. Figure 6 shows the simulation of change in slant column calculated from the observed vertical profile with and without photochemistry and Figure 7 (left) the impact on the retrieved mixing ratio. In the worst cases, August and March in the Arctic, the photochemical change results in a maximum error of 0.17 pptv, while it is even smaller in the Arctic winter (28 January) because of the slow drop of the BrO concentration in absence of NOx.

[33] The last concern regarding the measurement of BrO in the UV is the contribution of scattered sunlight. We have already seen that the data recorder in the presence of clouds are easily removed by looking at the CI. The impact of Rayleigh scattering in the field of view of the instrument has been simulated using the photochemical model [*Chipperfield*, 1999] coupled with a radiation transfer model including multiple scattering. The corresponding change in slant column for the flight of 20 March 1997 at Kiruna is shown in Figure 6, while the error on mixing ratios for extreme cases (winter and summer Arctic at low Sun) are shown in Figure 7. The impact of scattering results in errors on daytime BrO mixing ratios smaller than 0.3–0.4 pptv.

2.4. Conclusions and Error Summary

[34] The SAOZ-BrO instrument allows reliable measurements of the BrO profile from cloud top to float altitude during the daytime ascent of the balloon up to 88° SZA at

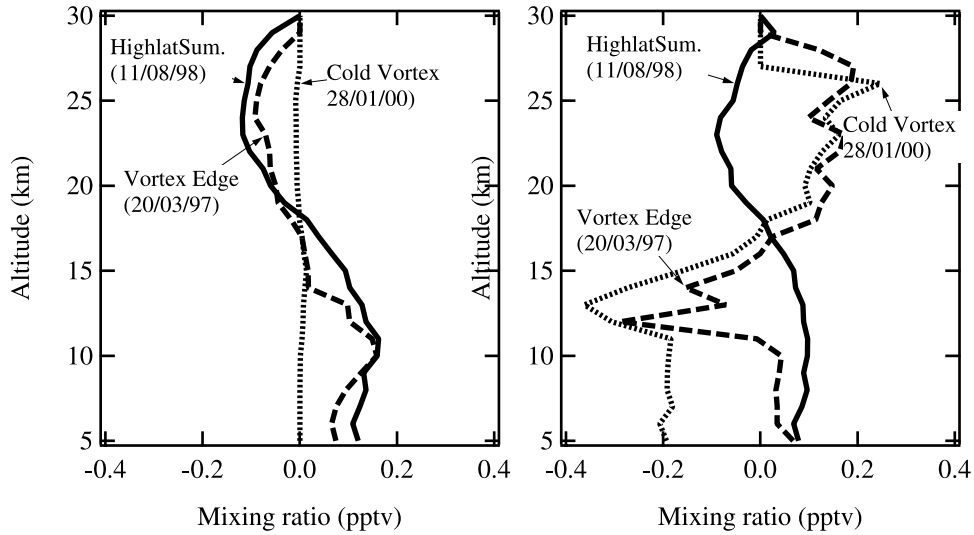

Figure 7. Change of BrO mixing ratio profiles by introducing photochemical change (left) and scattered light and photochemical change together (right) for selected extreme cases.

Table 3. Summary of Precision of Daytime BrO Mixing Ratio (ppt, One Standard Deviation)

Alt./Lat	W. Arct.	S. Arct.	W. Midlat.	S. Midlat.	Tropics
30 km	2.1	4.7	4.1	3.5	3.4
25 km	1.5	2.1	1.9	2.3	2.1
20 km	0.9	1.2	1.1	1.7	1.7
15 km	0.8	0.9	0.8	1.5	1.5
10 km	0.8	0.8	0.7	1.4	1.4

midlatitude and at the tropics and 89°–90° SZA in the Arctic. Indeed, because of the recombination of BrO into $BrONO_2$ at sunset, the more sensitive twilight occultation technique applied to other species cannot be used for BrO. The three components dominating the error budget are (1) the SZA-dependent precision of the slant column density, given for each measurement by the spectral fit, (2) the altitude-dependent impact of the error in the evaluation of the BrO residual amount in the reference spectrum, and (3) the systematic error of the BrO absorption cross sections measured in the laboratory and of their temperature dependence. Compared to those, the contribution of photochemical change and scattered sunlight could be neglected. As a result, the error budget is latitude and altitude dependent. The average figures of precision (one standard deviation) for each case are summarized in Table 3 to which a +5/−10% uncertainty due to the uncertainty on the BrO absorption cross sections has to be added for total accuracy. In addition, provision should be made for a temperature dependence if different from 223 K, estimated to 0.4%/K. Given the precision of the GPS, the uncertainty in the altitude registration is smaller than 100 m.

3. Flight Results

[35] Since the development of the new SAOZ-BrO sonde in 1997, it has been flown 16 times in the frame of several European projects (Stratospheric Regular Sounding in 1997–1998, THESEO-Stratospheric BrO and THESEO-Ozone Loss in 1998–2000). Altogether, they have allowed to explore the Arctic and midlatitudes at all seasons and also to perform a first flight at the tropics in Brazil. The BrO payload was always flown in "piggyback" below the regular SAOZ sonde, which provides more accurate ozone and NO_2 measurements in the visible part of the spectrum. Since only a lightweight two channel telemetry is generally used on small balloons to leave the maximum weight for scientific instruments, the data of the SAOZ-BrO are generally not transmitted in real time but are recorded in memory and thus available only after recovery. However, the BrO payload is autonomous, meaning that it has its own GPS altitude/location as well as Vaisala temperature (0.5 K accuracy) and pressure (1 hPa accuracy) sensors.

[36] These are required for profile inversion, and for conversion of number density, the primary product, into mixing ratio, which is more appropriate for chemical studies. Both presentations will be used in the following.

[37] The information relative to the 16 SAOZ/SAOZ-BrO flights is summarized in Table 4. In the Arctic these are performed from ESRANGE, the facility of Swedish Space Corporation at Kiruna at 68°N in northern Sweden and from the Norwegian Space Centre of Andoya at 69°N on the Norwegian coast. At midlatitudes they are carried from the ranges of the French Centre National d'Etudes Spatiales (CNES) at Aire sur l'Adour, 43°N (winter) and Gap, 44°N (summer). Finally one flight was performed from Brazil, at Bauru, 22°S, the balloon facility of the Istituto de Pesquisas Meteorologicas (IPMET) of the State University of São Paulo (UNESP).

[38] All flights were carried out in the afternoon. Depending on the total load, balloons of 5000 or 10000 m^3 were used which can carry 90 kg (60 kg of scientific instruments) to 27 km, and 120 kg (90 kg) to 30 km, respectively. Only one flight failed: the first on 24 February 1997 after the separation of the upper part of the optical head during launch operations. This was changed for a more robust arrangement for subsequent flights. Also shown in Table 4 is the balloon location with respect to the vortex (in, edge or out), and the state of chlorine activation derived from the presence of OClO at occultation for the winter Arctic

Table 4. Date and Location of the SAOZ-BrO Flights

Date	Location	Latitude	Vortex	SZA at 15 km	SZA at float	SZA noon
24/02/97	Kiruna, Sweden	68°N	In, activated	86°	88.8°	78°
20/03/97	Kiruna, Sweden	68°N	Edge	86°	88.5°	69°
24/06/97	Gap, France	44°N		83°	88.5°	21°
29/11/97	Bauru, Brazil	22°S		78°	87.3°	01°
02/03/98	Andoya, Norway	69°N	In, inactivated	84°	86.2°	76°
11/08/98	Kiruna, Sweden	68°N		87°	89.5°	53°
28/08/98	Kiruna, Sweden	68°N		86°	90.1°	58°
02/12/98	Aire, France	43°N		82°	87.5°	66°
27/01/99	Kiruna, Sweden	68°N	In, inactivated	88°	89.5°	87°
06/02/99	Kiruna, Sweden	68°N	In, inactivated	87°	89.5°	85°
22/04/99	Aire, France	43°N		82°	88.5°	31°
06/07/99	Gap, France	44°N		80°	84.7°	21°
28/01/00	Kiruna, Sweden	68°N	In, activated	87°	88.5°	87°
09/02/00	Kiruna, Sweden	68°N	Out	87°	91.6°	84°
13/02/00	Kiruna, Sweden	68°N	In, activated	87°	90.8°	82°
07/03/00	Kiruna, Sweden	68°N	In, activated	85°	87.6°	73°

Also indicated for the winter Arctic are the location with respect to the vortex (In, Edge, Out) and the chlorine activation as indicated by OClO (activated or warm). Also reported are the SZA at 15 km during the balloon ascent, when reaching float altitude and at noontime.

flights. Also indicated are the SZA at 15 km during the ascent, when the balloon is reaching float altitude, as well as at noontime, an important parameter for chemistry. In any case the BrO data at SZA > 90° are not used. The profile stops at the altitude where the SZA reaches 90°. Among the 15 flights providing good results, six have been carried out in the spring–summer season (2 in the Arctic, 3 at midlatitude, and 1 at the tropics) and the other ten in the winter (9 in the Arctic and 1 at midlatitude).

3.1. Summary of Results

[39] The 15 BrO profiles are displayed in Figure 8 in number density on the left, and in mixing ratio on the right, versus altitude, respectively. The approximate scales for the potential temperature levels are added. BrO is always present during daytime. In contrast to chlorine, a large fraction of inorganic bromine is in the form of BrO at all latitudes and all seasons. Its concentration shows a maximum in the lower stratosphere at an altitude varying from 15 km in the winter polar vortex to 20–22 km at midlatitudes in the summer and at the tropics. Its mixing ratio increases steadily from the tropopause up to 500–600 K in the winter and to 700–800 K in the summer, above which it remains constant at 12–15 pptv up to the maximum altitude of the measurements. Since the total concentration of inorganic bromine is of the order of 20 pptv, BrO would therefore represent on average about 60–70% of the total bromine during daytime in the midstratosphere. These observed BrO concentrations are globally consistent with that inferred by a photochemical model, i.e., in Figure 5, suggesting that stratospheric bromine chemistry be relatively well understood. The variability of the concentration is relatively small (±15%) in the vortex, but larger in the summer, in the Arctic as well as at midlatitudes. The winter midlatitude mixing ratio is very similar to that observed at the same season in the Arctic outside the vortex. Finally, in the series of flights, only two show detectable amounts of BrO at, and below, the altitude of the tropopause: one in July at midlatitudes when the tropopause was unusually low (10 km, 320 K) and the tropical one where the tropopause was at 17 km (380 K). Some specific and

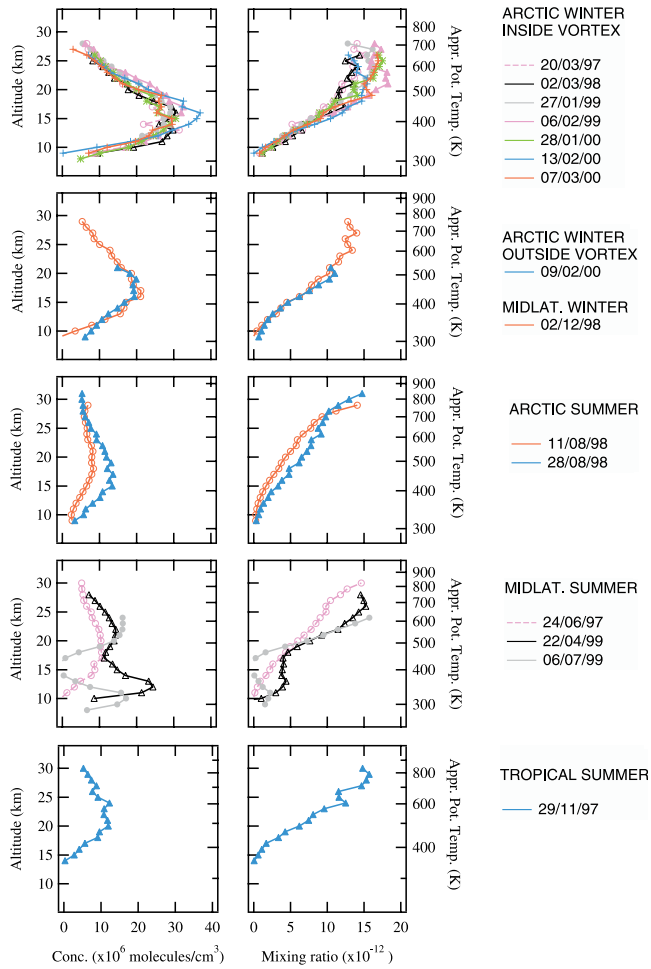

Figure 8. Summary of BrO profiles observed during the 15 balloon flights. Left: number density versus altitude, Right: mixing ratio versus altitude. From top to bottom: Arctic winter vortex, high latitude and midlatitude winter, Arctic summer, midlatitude summer, and tropics.

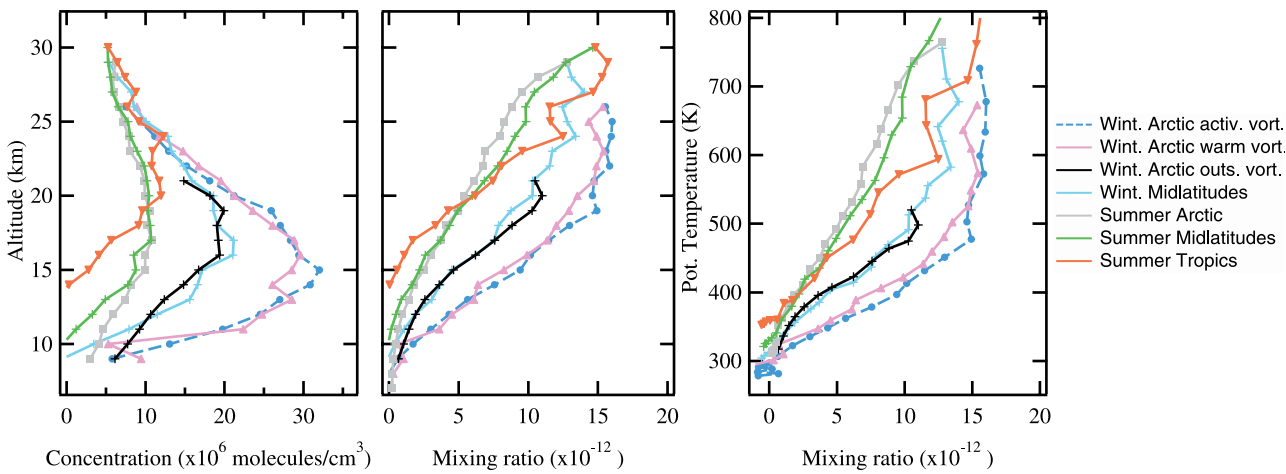

Figure 9. Average BrO profiles for each case of Figure 8. Left: concentration versus altitude. Middle: mixing ratio versus altitude. Right: mixing ratio versus potential temperature.

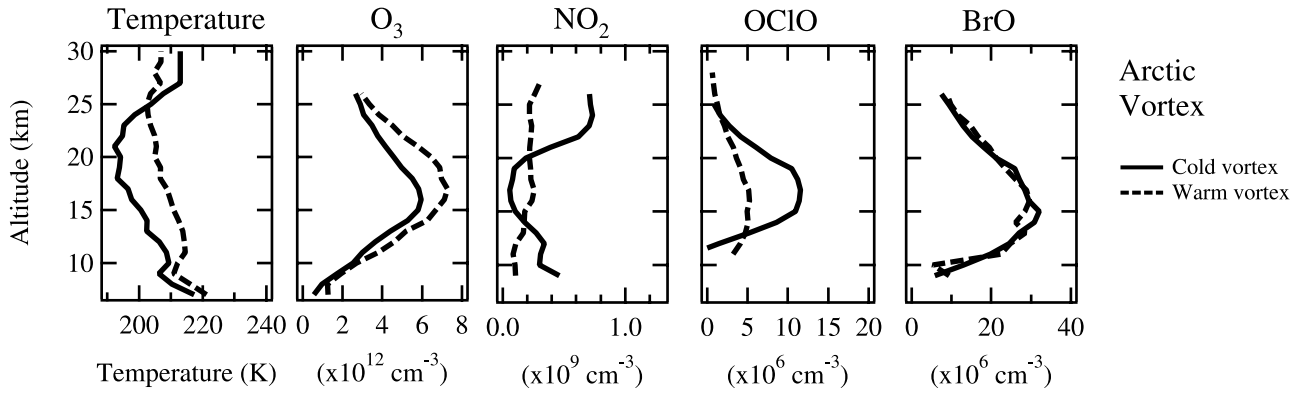

Figure 10. Average vertical distribution of temperature, sunset ozone, NO_2 and OClO and daytime BrO observed by the regular SAOZ and the SAOZ-BrO flown on the same balloon in the cold chlorine activated winter vortex of 2000 (full lines) and in warmer conditions in 1998 and 1999 (dotted).

intriguing characteristics of these results are explored in more detail below.

3.2. Seasonal and Latitudinal Change

[40] Figure 9 shows averaged profiles for each season and latitude, except the two strange summer midlatitude profiles associated with an abnormally low tropopause, which will be discussed later. A large part of the concentration and altitude changes seen in the left panel could be explained by the seasonal/latitudinal vertical displacements of the stratosphere. The larger concentration and lower altitude of the maximum number density in the vortex compared to the outside, just corresponds to the wintertime diabatic descent of 5 km following the cooling of the stratosphere. Similarly, the higher altitude and lower concentration at the tropics could be largely explained by the stratospheric uplift in this region. However, the BrO mixing ratio is not constant on a potential temperature surface. For example, and though the uncertainty is relatively larger there because of the high Sun, BrO is more abundant at a given potential temperature at the tropics than in the summer at mid and high latitudes. Chemistry also contributes which will be explored now by looking more closely at specific cases.

3.3. Impact of Chlorine Activation

[41] Figure 10 shows average daytime BrO profiles together with OClO, NO_2, ozone measured during occultation and temperature observed during the same flight by the regular SAOZ in the cold vortex of 2000 (full lines) compared to the average warm conditions of the 1998 and 1999 (dotted). As a result of the cold temperature, significant amounts of OClO, indicative of chlorine activation, were observed at sunset between 14 and 20 km in 2000 but much less in the previous years. NO_2 is depleted in 2000 in the same altitude range due to denoxification on PSCs (and possibly to denitrification), but increases above 20 km because of the later date of the flights in 2000. It increases also below 14 km, possibly because of the redistribution of NO_x after the sedimentation of PSC particles [*Goutail et al.*, 2001]. Finally, ozone was significantly depleted in 2000 compared to previous years (F. Goutail et al., Total ozone loss in the Arctic winter vortex of 2000 and comparison to previous years, submitted to *Journal of Geophysical Research*, 2002). In contrast, BrO concentrations are identical in 1998–1999 and 2000. These results suggest that PSCs and chlorine activation have little impact on daytime bromine, although the partitioning of nighttime reservoirs is likely to be strongly modified in favor of BrCl.

3.4. Summer Arctic

[42] Two flights have been performed in similar meteorological conditions (light wind in the stratosphere) during the same month during the Arctic summer of 1998, the first on 11 August, and the second on 28 August. Their respective temperature, ozone, NO_2, and daytime BrO profiles are displayed in the top panels of Figure 11. Though the temperature and ozone did not vary between the two dates, the NO_2 amount has dropped by 20–30%. Indeed the NOx concentration, maximum during the polar day, drops as the duration of the night increases (6h30 on 28 August instead of 3h10 on 11 August at SZA > 95°) because of the nighttime formation of N_2O_5 followed by its hydrolysis into nitric acid [*Pommereau and Goutail*, 1988]. The change in BrO is just the opposite. The decrease of NO_2 impacts the partitioning between BrO and $BrONO_2$. The concentration of the latter, maximum during the polar day drops rapidly in late summer. As can be seen in Figure 11, the location and season where BrO is relatively the least abundant is the Arctic summer.

3.5. BrO Variability in the Summer Midlatitude

[43] Surprisingly the BrO profiles observed in late spring and early summer over southern France are highly variable. In two cases, a BrO-rich layer is observed at or immediately above the tropopause. The middle panels of Figure 11 show that these are not due to measurement errors since similar features could be observed on O_3 and NO_2, but rather to transport or mixing. The minimum BrO in June 1997 is associated with a typical summer meteorological situation (tropopause around 12 km, easterly wind in the stratosphere), and a maximum NO_2 (consistent with $BrONO_2$ formation as explained earlier). The late spring BrO double peak profile of 22 April 1999 exactly mimics the double peak distribution of ozone, frequent during spring, and indicative of large-scale transport of air from high latitude in the lower stratosphere.

[44] Finally, the BrO-rich layer in the upper troposphere and the lower stratosphere on 6 July 1999 is also rich in

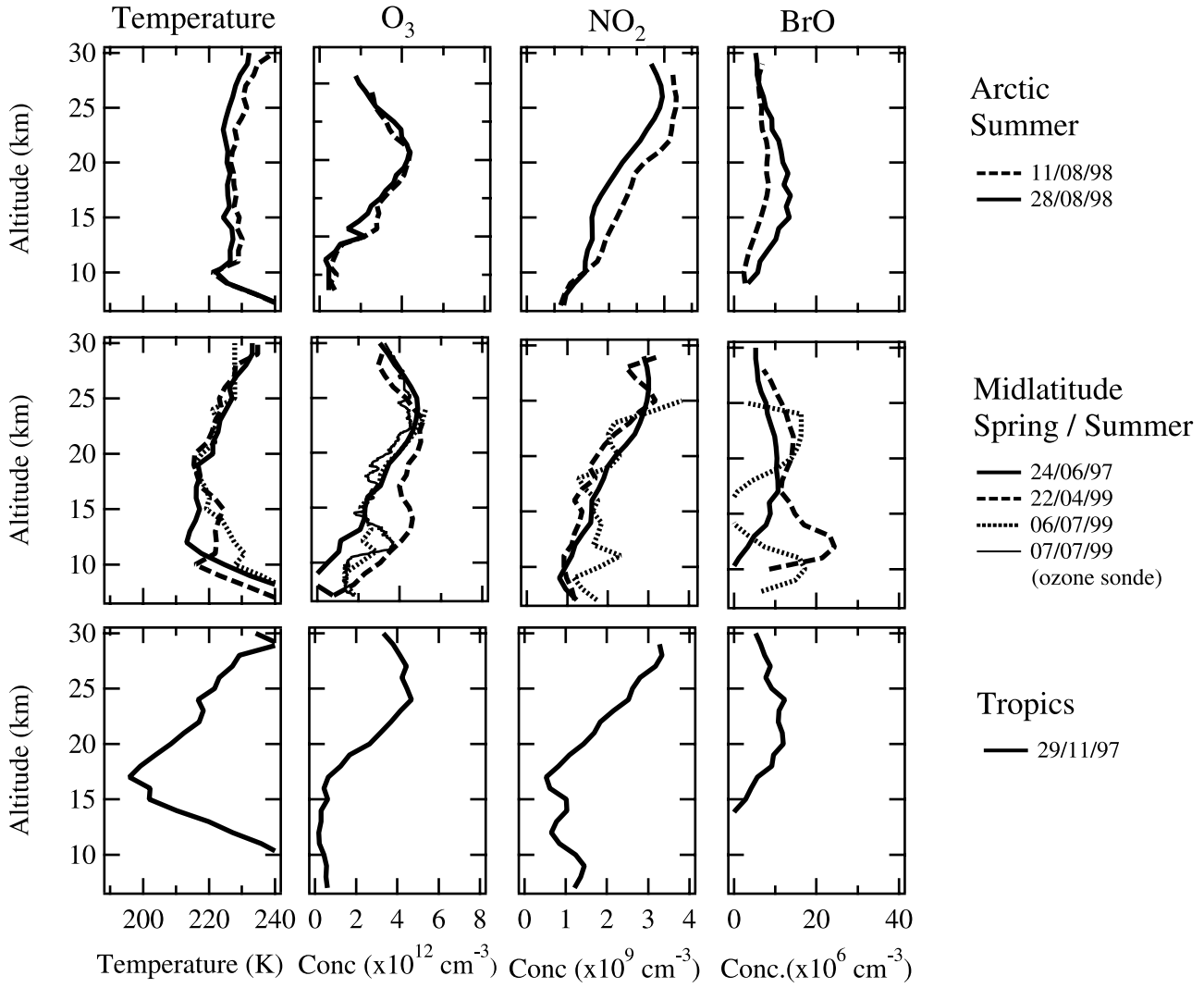

Figure 11. Temperature, sunset ozone, and NO_2 and daytime BrO: (a) over Kiruna on 11 and 28 August 1998, (b) over southern France in spring and summer. Full: 24 June 1997; dashed: 22 April 1999; dotted: 6 July 1999 (also shown: ozonesonde on 25 April), and (c) at 22°S over Brazil on 29 November 1997.

NO_2 and ozone, as confirmed by an ozone sonde launched from the same place on the following day. It corresponds to a particularly strong cutoff low event centered over France according to pressure charts of Meteo-France (not shown) and to a drop of tropopause altitude as low as 280 hPa in the radiosonde at Nimes at 12 UT. It is the signature of a stratosphere–troposphere exchange (STE) event, advecting stratospheric air rich in O_3, NO_2, and BrO into the troposphere. The observed BrO-depleted layer above is therefore likely the signature of tropospheric air entering into the stratosphere. In addition to the seasonal and latitudinal changes, the BrO vertical distribution is also sensitive to short term vertical transport of total inorganic bromine.

3.6. Summer Tropics

[45] The tropical flight of 29 November 1997 was performed from Bauru at 22°S, 300 km west of the city of São Paulo, over an area of deep convection in the summer. As shown in the lower panels of Figure 11 the tropopause is raised to 17 km and both stratospheric species, ozone and NO_2, show a sharp discontinuity at this level. In contrast, the BrO abundance does not: BrO is still present in the uppermost troposphere. The suggested explanation for this behavior, consistent with the altitude of the BrO peak concentration being lower than that of ozone, is the partial conversion of organic bromine into inorganic forms in the upper troposphere at very high Sun before entering into the stratosphere. Since the vertical transport across the tropical tropopause is a slow process, it is possible that these inorganic degradation products could never enter into the stratosphere. Another indication could be that, in contrast to ozone and NOx, cirrus or anvils of cumulonimbus clouds frequent in this area would not deplete BrO. However, additional flights would be required to confirm these suggestions.

3.7. Comparison to Other Measurements

[46] The only place where significant comparisons could be performed is the wintertime Arctic, where three different techniques have been used: balloon-borne in situ resonance fluorescence [*McKinney et al.*, 1997; *Stroh et al.*, 1998],

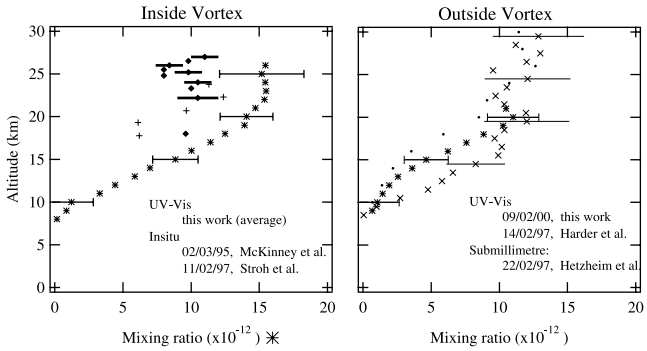

Figure 12. BrO profiles measured over Kiruna in the winter by balloon-borne UV–visible spectroscopy, balloon-borne in situ resonance–fluorescence, and airborne submillimetric spectroscopy, inside (left) and outside (right) the vortex. Error bars shown at few levels only for clarity. Explanations in Table 5.

balloon UV–visible spectroscopy [*Harder et al.*, 1998; this work] and remote sensing by submillimeter spectroscopy from an aircraft [*Hetzheim et al.*, 1998]. Though the measurements by different techniques are not at the same local time and even not on the same year, some meaningful comparisons could be obtained by just separating the data set between the inside and the outside of the vortex. Indeed we have seen previously that the major cause of change of BrO concentration in the Arctic winter is the vertical displacement of total bromine between the inside and the outside and not the state of activation of chlorine (Figure 8).

[47] Figure 12 shows the comparison of available results in the vortex on the left and outside on the right (for details, see Table 5). All daytime profiles show an increase of the BrO mixing ratio above the tropopause at 7–10 km up to an altitude (around 20 km), above which it remains approximately constant up to the top altitude of observations at 25–30 km. Outside the vortex, the three remote sensing measurements (two UV–visible and one submillimeter) are consistent with each other within their respective uncertainties (when known) above 20 km where the BrO mixing ratio is constant and therefore insensitive to local vertical displacement of the stratosphere. Inside the vortex, where the BrO profile was found very similar from one winter to the other in the SAOZ BrO measurements, the two low Sun (90°–92° SZA) sunrise in situ observations of McKinney et al., and the daytime (SZA < 83°) balloon measurements of Stroh et al. are consistent with each other but suggest lower concentration than those derived by the UV–visible instrument. However, a large part of the apparent discrepancy could be explained by the uncertainty of the BrO absorption cross section in the UV (−5/+10%), the uncertainty of its temperature dependence, and the different local time and SZA of the measurements. Though of small amplitude, another contribution is the change of total bromine concentration, which is expected to have increased by 1.5 ppt between 1995 and 2000. A better assessment of possible systematic differences between the two techniques would require a comparison of measurements performed at same local time and SZA, as well as a better characterization of BrO cross sections at low temperature.

4. Summary and Conclusions

[48] A balloon-borne UV–visible spectrometer, the SAOZ-BrO, has been designed for the measurement of BrO abundances on frequent and relatively inexpensive small balloon flights. The instrument allows the retrieval of the BrO vertical profile with a vertical resolution of 1.4 km, an average precision of 0.5–2 pptv and accuracy of +5/−10% but during the daytime ascent of the balloon only. Indeed because of the fast photochemical decay of BrO at sunset, the solar occultation technique from float altitude at twilight used for other species could not be employed. Fifteen successful flights have been carried out since the maiden flight of the instrument in 1997, in the Arctic and midlatitude winter and summer as well as at the tropics. Significant BrO concentrations were observed everywhere in the daytime in the stratosphere with a peak concentration altitude varying from 15 km in the winter vortex to 22 km at the tropics. The BrO mixing ratio increases steadily from the tropopause to 25–30 km, depending on the latitude and the season, above which it remains constant up to the top altitude of the observations, at about 30 km. At these levels, BrO is the most abundant bromine species during daytime which would represent on average about 60–70% of the total inorganic bromine. The consistence of this figure with model simulations suggests that stratospheric bromine chemistry be relatively well understood.

[49] The latitudinal and seasonal changes of BrO concentration are largely controlled by the vertical transport of total inorganic bromine at all timescales and to a smaller extent by photochemistry. Photochemical changes are primarily related to the abundance of NO_2. At constant potential temperature, the BrO mixing ratio is the largest in the winter polar vortex area, because of air subsidence but also of the low NO_2 at low Sun and denoxification on PSC particles. At the opposite, the BrO mixing ratio is the smallest during the permanent polar day and at midlatitude in the summer where the NO_2 concentration is the largest. Likely because of the relatively small NO_2 abundance, the BrO mixing ratio at constant potential temperature is larger at the tropics than at midlatitude in the summer.

[50] The comparison of wintertime Arctic measurements at cold and warm temperature suggests that the presence of

Table 5. Detail of Data Sets, SZA Range, and Error Bars Shown in Figure 12

	SZA	BrO data	Uncertainty, error bars
McKinney et al. [1997]	90°–92° sunrise	Lowest data point omitted (error > 10 ppt)	Total accuracy (2 σ)
Stroh et al. [1998]	<83°	Ascent and descent averaged for clarity	50%, preliminary error bars not shown
Hetzheim et al. [1998]	<85° (11–13 UT)	All data	Uncertainty unknown
Harder et al. [1998]	<88°	All data	Total accuracy (2 σ) BrO cross section not included
This work	84°–90°	All vortex flights averaged only one profile out of vortex	Total accuracy (2 σ) BrO cross section not included

activated chlorine in the cold vortex has negligible impact on the daytime abundance of BrO. Though these different conditions would be expected to cause large differences in the abundances of the BrO nighttime reservoirs.

[51] Finally, significant amounts of BrO were observed at two occasions in the upper troposphere: (1) in the summer at midlatitude where it was the result of a STE event advecting bromine together with ozone and NOx from the stratosphere and (2) at tropics where its presence is more likely due to the conversion of organic bromine at high Sun.

[52] **Acknowledgments.** The authors thank Pierre François for his work in building the SAOZ-BrO payload and the teams of the Centre National d'Etudes Spatiales, the Swedish Space Corporation, the Norwegian Space Centre, and the Institute of Meteorological Research of the State University of São Paulo for successful balloon operations. Also acknowledged are Caroline Fayt for advises for using WINDOAS, Andreas Richter and Thomas Wagner for helpful discussions, and the three anonymous reviewers for their excellent comments. This work was supported by the French Programme National de Chimie de l'Atmosphère (PNCA), the Belgian SSTC and the FNRS, and the several projects of the Research Direction Générale of the European Commission: Stratospheric Regular Sounding (ENV4-CT95-0040), Stratospheric BrO (ENV4-CT97-0521), and Eurosolve (EVK2-1999-00311). I. Pundt was holding a fellowship of the European Commission.

References

Aliwell, S. R., R. L. Jones, and D. J. Fish, Mid-latitude observations of the seasonal variation of BrO, 1, Zenith-sky measurements, *J. Geophys. Res.*, *24*, 1195–1198, 1997.

Aliwell, S. R., et al., Analysis for BrO in zenith-sky spectra: An intercomparison exercise for analysis improvement, *J. Geophys. Res.*, *107*(D14), 4199, doi:10.1029/2001JD000329, 2002.

Arpag, K. H., P. V. Johnston, H. L. Miller, R. W. Sanders, and S. Solomon, Observations of the stratospheric BrO column over Colorado, 40°N, *J. Geophys. Res.*, *99*, 8175–8181, 1994.

Avallone, L. M., D. W. Toohey, S. M. Schauffler, W. H. Pollock, L. E. Heidt, E. L. Atlas, and K. R. Chan, In situ measurements of BrO during AASE II, *Geophys. Res. Lett.*, *22*, 831–834, 1995.

Brune, W. H., and J. G. Anderson, In situ observations of mid latitude stratospheric ClO and BrO, *Geophys. Res. Lett.*, *13*, 1391, 1986.

Brune, W. H., J. G. Anderson, and K. R. Chan, In situ observations of BrO over Antarctica: ER-2 aircraft results from 54°S to 72° latitude, *J. Geophys. Res.*, *94*, 16,649, 1989.

Burrows, J. P., et al., The Global Ozone Monitoring Experiment (GOME): Mission concept and first scientific results, *J. Atmos. Sci.*, *56*, 151–175, 1999a.

Burrows, J. P., A. Richter, A. Dehn, B. Deters, S. Himmelmann, S. Voigt, and J. Orphal, Atmospheric remote-sensing reference data from GOME, 2, Temperature-dependent absorption cross sections of O_3 in the 231–794 nm range, *J. Quant. Spectrosc. Radiat. Transfer*, *61*, 509–517, 1999b.

Carroll, M. A., R. W. Sanders, S. Solomon, and A. L. Schmeltekopf, Visible and near-ultraviolet spectroscopy at McMurdo station, Antarctica, 6, Observations of BrO, *J. Geophys. Res.*, *94*, 16,633, 1989.

Chipperfield, M., Multiannual simulations with a three-dimensional chemical transport model, *J. Geophys. Res.*, *104*, 1781–1805, 1999.

Daniel, J. S., S. Solomon, R. W. Portmann, and R. R. Garcia, Stratospheric ozone destruction: The importance of bromine relative to chlorine, *J. Geophys. Res.*, *104*, 23,871–23,880, 1999.

Dvortsov, V. L., M. A. Geller, S. Solomon, S. M. Schauffler, E. L. Atlas, and D. R. Blake, Rethinking reactive halogen budget in the midlatitude stratosphere, *Geophys. Res. Lett.*, *26*, 1699–1702, 1999.

Fish, D. J., S. R. Aliwell, and R. L. Jones, Mid-latitude observations of the seasonal variation of BrO, 2, Interpretation and modelling study, *Geophys. Res. Lett.*, *24*, 1199–1202, 1997.

Fitzenberger, R., H. Bösch, C. Camy-Peyret, M. P. Chipperfield, H. Harder, U. Platt, B.-M. Sinnhuber, T. Wagner, and K. Pfeilsticker, First profile measurements of tropospheric BrO, *Geophys. Res. Lett.*, *27*, 2921–2924, 2000.

Fraser, P., D. Oram, C. Reeves, and S. Penkett, Southern Hemispheric halon trends (1978–1998) and global halon emissions, *J. Geophys. Res.*, *104*, 15,985–15,999, 1999.

Friess, U., M. P. Chipperfield, H. Harder, C. Otten, U. Platt, J. Pyle, T. Wagner, and K. Pfeilsticker, Intercomparison of measured and modelled BrO slant column amounts for the Arctic winter and spring 1994/95, *Geophys. Res. Lett.*, *26*, 1861–1864, 1999.

Garcia, R. R., and S. Solomon, A new numerical model of the middle atmosphere, 2, Ozone and related species, *J. Geophys. Res.*, *99*, 12,937–12,951, 1994.

Gilles, M. K., A. A. Turnipseed, J. B. Burkholder, A. R. Ravishankara, and S. Solomon, Kinetics of the IO radical, 2, Reaction of IO with BrO, *J. Phys. Chem.*, *101*, 5526–5534, 1997.

Goutail, F., et al., Total ozone depletion in the Arctic during the winters of 1993–94 and 1994–95, *J. Atmos. Chem.*, *32*, 1–34, 1999.

Goutail, F., L. Denis, J. P. Pommereau, F. Lefevre, and C. Deniel, Ozone loss, NO_x and chlorine during the arctic winter of 1999–2000 as reported by SAOZ ground-based, short and long duration balloon flights, in *Proc. 15th ESA Symp. Eur. Rocket and Balloon, ESA SP*, vol. 471, pp. 239–244, Eur. Space Agency, Noordwicjk, Netherlands, 2001.

Grendel, A., A. Grund, and D. Perner, Transall DOAS-measurements of stratospheric OClO, BrO, NO_2 and O_3 in winter 1994/95, in *Proc. 3rd Eur. Polar Ozone Symp., EC Air Pollut. Res.*, vol. 56, edited by J. A. Pyle et al., pp. 319–322, Eur. Comm., Brussels, Belgium, 1996.

Harder, H., et al., Stratospheric BrO profiles measured at different latitudes and seasons, 2, Atmospheric observations, *Geophys. Res. Lett.*, *25*, 3843–3846, 1998.

Harder, H., H. Bösch, C. Camy-Peyret, M. Chipperfield, R. Fitzenberger, S. Payan, D. Perner, U. Platt, B.-M. Sinnhuber, and K. Pfeilsticker, Comparison of measured and modelled stratospheric BrO: Implications for the total amount of stratospheric bromine, *Geophys. Res. Lett.*, *27*, 3695–3698, 2000.

Hegels, E., P. J. Crutzen, T. Kluepfel, and D. Perner, Global distribution of atmospheric bromine-monoxide from GOME on earth observing satellite ERS-2, *Geophys. Res. Lett.*, *25*, 3127–3130, 1998.

Hetzheim, H., G. Schwaab, V. Eyring, H. Küllmann, K. Künzi, J. Urban, A. P. H. Goede, A. de Jonge, Q. L. Kleipool, and N. D. Whyborn, A new method to retrieve profiles of minor atmospheric constituents and its application to the '97 ASUR campaign, in *Proc. 4rd Eur. Polar Ozone Symp., EC Air Pollut. Res. Rep.*, vol. 66, edited by N. R. P. Harris et al., pp. 669–672, Eur. Comm., Brussels, Belgium, 1998.

Johnson, D. G., W. A. Traub, K. V. Chance, and K. W. Jucks, Detection of HBr and upper limit for HOBr: Bromine partitioning in the stratosphere, *Geophys. Res. Lett.*, *22*, 1373, 1995.

Ko, M., N. Sze, C. Scott, and D. Weisenstein, On the relation between chlorine/bromine loading and short-lived tropospheric source gases, *J. Geophys. Res.*, *102*, 25,507–25,517, 1997.

Kreher, K., P. V. Johnston, S. Wood, B. Nardi, and U. Platt, Ground-based measurements of tropospheric and stratospheric BrO at Arrival Heights, Antarctica, *Geophys. Res. Lett.*, *24*, 3021–3024, 1997.

Kurucz, R. L., I. Furenlid, J. Brault, and L. Testerman, Solar flux atlas from 296 nm to 1300 nm, *National Solar Observatory Atlas 1*, 1984.

Lary, D. J., Gas phase atmospheric bromine photochemistry, *J. Geophys. Res.*, *101*, 1505–1516, 1996.

Lary, D. J., M. P. Chipperfield, R. Toumi, and T. Lenton, Heterogeneous atmospheric bromine chemistry, *J. Geophys. Res.*, *101*, 1489–1504, 1996.

McElroy, M. B., R. J. Salawitch, S. C. Wofsy, and J. A. Logan, Reductions of Antarctic ozone due to synergistic interactions of chlorine and bromine, *Nature*, *321*, 759–762, 1986.

McElroy, C. T., C. A. McLinden, and J. C. McConnel, Evidence for bromine monoxide in the free troposphere during the Arctic polar sunrise, *Nature*, *397*, 338–341, 1999.

McKinney, K. A., J. M. Pierson, and D. W. Toohey, A wintertime in situ profile of BrO between 17 and 27 km in the Arctic vortex, *Geophys. Res. Lett.*, *24,8*, 853–856, 1997.

Otten, C., F. Ferlemann, U. Platt, T. Wagner, and K. Pfeilsticker, Ground-based DOAS UV/visible measurements at Kiruna (Sweden) during the SESAME winters 1993/94 and 1994/95, *J. Atmos. Chem.*, *30*, 141–162, 1998.

Nolt, I. G., et al., Stratospheric HBr concentration profile obtained from far-infrared emission spectroscopy, *Geophys. Res. Lett.*, *24*, 281–284, 1997.

Pfeilsticker, K., W. T. Sturges, H. Bösch, C. Camy-Peyret, M. P. Chipperfield, A. Engel, R. Fitzenberger, M. Müller, S. Payan, and B.-M. Sinnhuber, Lower stratospheric organic and inorganic bromine budget for the Arctic winter 1998/99, *Geophys. Res. Lett.*, *27*, 3305–3308, 2000.

Platt, U., Differential optical absorption spectroscopy (DOAS), in *Air Monitoring by Spectroscopic Techniques*, edited by M. W. Sigrist, pp. 27–84, John Wiley, New York, 1994.

Pommereau, J. P., and F. Goutail, O_3 and NO_2 ground-based measurements by visible spectrometry during arctic winter and spring 1988, *Geophys. Res. Lett.*, *15*, 891, 1988.

Pommereau, J.-P., and J. Piquard, Ozone and nitrogen dioxide vertical distributions by UV–visible solar occultation from balloons, *Geophys. Res. Lett.*, *21*, 1227–1230, 1994a.

Pommereau, J.-P., and J. Piquard, Observations of the vertical distribution of stratospheric OClO, *Geophys. Res. Lett.*, *21*, 1231–1234, 1994b.

Pommereau, J. P., et al., Small balloons for stratospheric ozone research and satellite validation, in *Proc. 14th ESA Symp. on European Rocket and Balloon Programmes, ESA SP*, vol. 437, pp. 609–614, Eur. Space Agency, Noordwicjk, Netherlands, 1999.

Pundt, I., Distribution verticale de la concentration de IO et de BrO dans la basse stratosphère: Mesure et interprétation, Ph.D. thesis, Univ. of Paris VI, Paris, 1997.

Pundt, I., J. P. Pommereau, and F. Lefèvre, Investigation of stratospheric bromine and iodine oxides using the SAOZ balloon sonde, in *Atmospheric Ozone. Proc. of the XVIII Quadrennial Ozone Symposium, L'Aquila, Italy, 12–21 September 1996*, vol. 2, edited by R. D. Bojkov and G. Visconti, pp. 575–578, Int. Ozone Comm., L'Aquila, Italy, 1997.

Pundt, I., J. P. Pommereau, C. Phillips, and E. Lateltin, Upper limit of iodine oxide in the lower stratosphere, *J. Atmos. Chem.*, *30*, 173–185, 1998.

Pundt, I., et al., Simultaneous UV–vis measurements of BrO from balloon, satellite and ground: Implications for tropospheric BrO, in *Proc. 5rd Eur. Polar Ozone Symp., CEC*, edited by N. R. P. Harris et al., pp. 316–319, Eur. Comm., Brussels, Belgium, 2000.

Richter, A., F. Wittrock, M. Eisinger, and J. P. Burrows, GOME observations of tropospheric BrO in Northern Hemispheric spring and summer 1997, *Geophys. Res. Lett.*, *25*, 2683–2686, 1998.

Richter, A., M. Eisinger, A. Ladstätter-Weißenmayer, and J. P. Burrows, DOAS zenith sky observations, 2, Seasonal variation of BrO over Bremen (53°N) 1994–1995, *J. Atmos. Chem.*, *32*, 83–99, 1999.

Richter, A., F. Wittrock, A. Ladtstätter-Weißenmayer, and J. P. Burrows, GOME measurements of stratospheric and tropospheric BrO, *Adv. Space Res.*, *29*(11), 1667–1672, 2002.

Schauffler, S. M., E. L. Atlas, F. Flocke, R. A. Lueb, V. Stroud, and W. Travnicek, Measurements of bromine containing organic compounds at the tropical tropopause, *Geophys. Res. Lett.*, *25*, 317–320, 1998.

Schauffler, S. M., E. L. Atlas, D. R. Blake, F. Flocke, R. A. Lueb, J. M. Lee-Taylor, V. Stroud, and W. Travnicek, Distributions of brominated organic compounds in the troposphere and lower stratosphere, *J. Geophys. Res.*, *104*, 21,513–21,535, 1999.

Sinnhuber, B.-M., et al., Intercomparison of measured and modeled slant column densities, *J. Geophys. Res.*, *107*(D19), 4398, doi:10.1029/2001JD000940, 2002.

Solomon, S., R. W. Sanders, M. A. Carroll, and A. L. Schmeltekopf, Visible and near-ultraviolet spectroscopy at McMurdo Station, 5, Observations of the diurnal variations of BrO and OClO, *J. Geophys. Res.*, *94*, 11,393–11,403, 1989.

Stroh, F., T. Woyke, D. Toohey, A. Engel, and T. Deshler, Results of 1996/97 in-situ measurements of halogen oxides in the mid-latitude and arctic stratosphere, in *Proc. 4rd Eur. Polar Ozone Symp., EC Air Pollut. Res. Rep.*, vol. 66, edited by N. R. P. Harris et al., pp. 389–392, Eur. Comm., Brussels, Belgium, 1998.

Sturges, W. T., D. E. Oram, L. J. Carpenter, S. A. Penkett, and A. Engel, Bromoform as a source of stratospheric bromine, *Geophys. Res. Lett.*, *27*, 2081–2084, 2000.

Toohey, D. W., J. G. Anderson, W. H. Brune, and K. R. Chan, In situ measurements of BrO in the arctic stratosphere, *Geophys. Res. Lett.*, *17*, 513–516, 1990.

Van Daele, A.-C., C. Hermans, P. C. Simon, M. Carleer, R. Colin, S. Fally, M.-F. Merienne, A. Jenouvrier, and B. Coquart, Measurements of the NO_2 absorption cross-section from 42,000 cm^{-1} to 10,000 cm^{-1} (238–1000 nm) at 220 K and 294 K, *J. Quant. Spectrosc. Radiat. Transfer*, *59*, 171–184, 1998.

Van Roozendael, M., C. Fayt, J.-C. Lambert, I. Pundt, T. Wagner, A. Richter, and K. Chance, Development of a bromine oxide product from GOME, in *Proc. ESAMS'99*, *European Symposium on Atmospheric Measurements from Space*, WPP-161, pp. 543–547, ESTEC, Noordwijk, Netherlands, 18–22 January 1999.

Van Roozendael, M., et al., Intercomparison of BrO measurements from ERS-2 GOME, ground-based and balloon platforms, *Adv. Space Res.*, *29*(11), 1661–1666, 2002.

Wagner, T., and U. Platt, Satellite mapping of enhanced BrO concentrations in the troposphere, *Nature*, *395*, 486–490, 1998.

Wagner, T., Satellite observation of atmospheric halogen oxides, Ph.D. thesis, Univ. of Heidelberg, Germany, 1999.

Wahner, A., A. R. Ravishankara, S. P. Sander, and R. R. Friedl, Absorption cross-section of BrO between 312 and 385 nm at 298 and 223K, *Chem. Phys. Lett.*, *152*, 507–512, 1988.

Wahner, A., G. S. Tyndall, and A. R. Ravishankara, Absorption cross sections for OClO as a function of temperature in the wavelength range 240–480 nm, *J. Phys. Chem.*, *91*, 2734–2738, 1987.

Wahner, A., J. Callies, H. P. Dorn, U. Platt, and C. Schiller, Near UV atmospheric absorption measurements of column abundances during airborne arctic stratospheric expedition, January–February 1989, 3, BrO-observations, *Geophys. Res. Lett.*, *17*, 517, 1990.

Wamsley, P. R., et al., Distribution of halon-1211 in the upper troposphere and lower stratosphere and the 1994 total bromine budget, *J. Geophys. Res.*, *103*, 1513, 1998.

Wennberg, P., et al., Removal of stratospheric O_3 by radicals: In situ measurements of OH, HO_2, NO, NO_2, ClO and BrO, *Science*, *266*, 398–404, 1994.

WMO: World Meteorological Organization/UNEP, *Scientific Assessment of Ozone Depletion: 1994*, Global Res. and Monit. Proj. Rep. 37, Geneva, Switzerland, 1995.

WMO: World Meteorological Organization/UNEP, *Scientific Assessment of Ozone Depletion: 1998*, Global Res. and Monit. Proj. Rep. 44, Geneva, Switzerland, 1999.

Wofsy, S. C., M. B. McElroy, and Y. L. Yung, The chemistry of atmospheric bromine, *Geophys. Res. Lett.*, *2*, 215, 1975.

Yung, Y. L., J. P. Pinto, R. T. Watson, and S. P. Sander, Atmospheric bromine and ozone perturbations in the lower stratosphere, *J. Atmos. Sci.*, *37*, 339–353, 1980.

M. P. Chipperfield, School of the Environment, University of Leeds, Leeds LS2 9JT, UK. (martyn@env.leeds.ac.uk)

F. Goutail and J.-P. Pommereau, Service d'Aéronomie, BP3, F-91371 Verrières-le-Buisson, France. (fgoutail@aerov.jussieu.fr; pommereau@aerov.jussieu.fr)

I. Pundt, Institute of Environmental Physics, University of Heidelberg, Im Neuenheimer Feld 229, D-69120 Heidelberg, Germany. (irene.pundt@iup.uni-heidelberg.de)

M. Van Roozendael, Belgian Institute for Space Aeronomy, Avenue Circulaire 3, B-1180 Brussels, Belgium. (Michel.Vanroozendael@oma.be)